

Electronic Supplementary Information

## Nitrogen and sulfur co-doped porous carbon derived from human hair as highly efficient metal-free electrocatalyst for hydrogen evolution reaction

Xiaojun Liu,<sup>a</sup> Weijia Zhou,<sup>\*a</sup> Linjing Yang,<sup>a</sup> Ligui Li,<sup>a</sup> Zhenyuan Zhang,<sup>a</sup> Yunting Ke,<sup>a</sup> and Shaowei Chen<sup>\*a,b</sup>

<sup>a</sup> *New Energy Research Institute, School of Environment and Energy, South China University of Technology, Guangzhou Higher Education Mega Center, Guangzhou, Guangdong 510006, China.*

<sup>b</sup> *Department of Chemistry and Biochemistry, University of California, 1156 High Street, Santa Cruz, California 95064, United States.*

*E-mails: eszhouwj@scut.edu.cn (W.J.Z.); shaowei@ucsc.edu (S.W.C).*

**Video S1.** Video of bubble formation on the HPC-800 electrode at the applied potential of -0.15V (vs. RHE).

**Table S1.** Summary of textural parameters obtained from nitrogen adsorption analysis of samples

Samples	$S_{\text{BET}}$ ( $\text{m}^2 \text{g}^{-1}$ )	Pore volume ( $\text{cm}^3 \text{g}^{-1}$ )	Pore size (nm)
HPC-600	535.2	0.37	31.5
HPC-700	597.3	0.40	34.1
HPC-800	830.0	0.88	51.1
HPC-900	617.8	0.65	37.6

**Table S2.** N and S dopant concentrations in the porous carbons determined by XPS measurements.

	Pyrrolic-N (at.%)	Pyridinic-N (at.%)	Graphitic-N (at.%)	C-S-C (at.%)	C=S (at.%)	C-SO <sub>x</sub> -C (at.%)	
						<i>x</i> = 2	<i>x</i> = 3
HPC -600	2.54	2.29	0.28	0.49	0.09	0.27	0.27
HPC -700	1.39	1.87	0.94	0.32	0.14	0.24	0.21
HPC -800	0.68	1.02	1.81	0.19	0.30	0.08	0.16
HPC -900	0.21	0.45	1.47	0.29	0.12	—	—

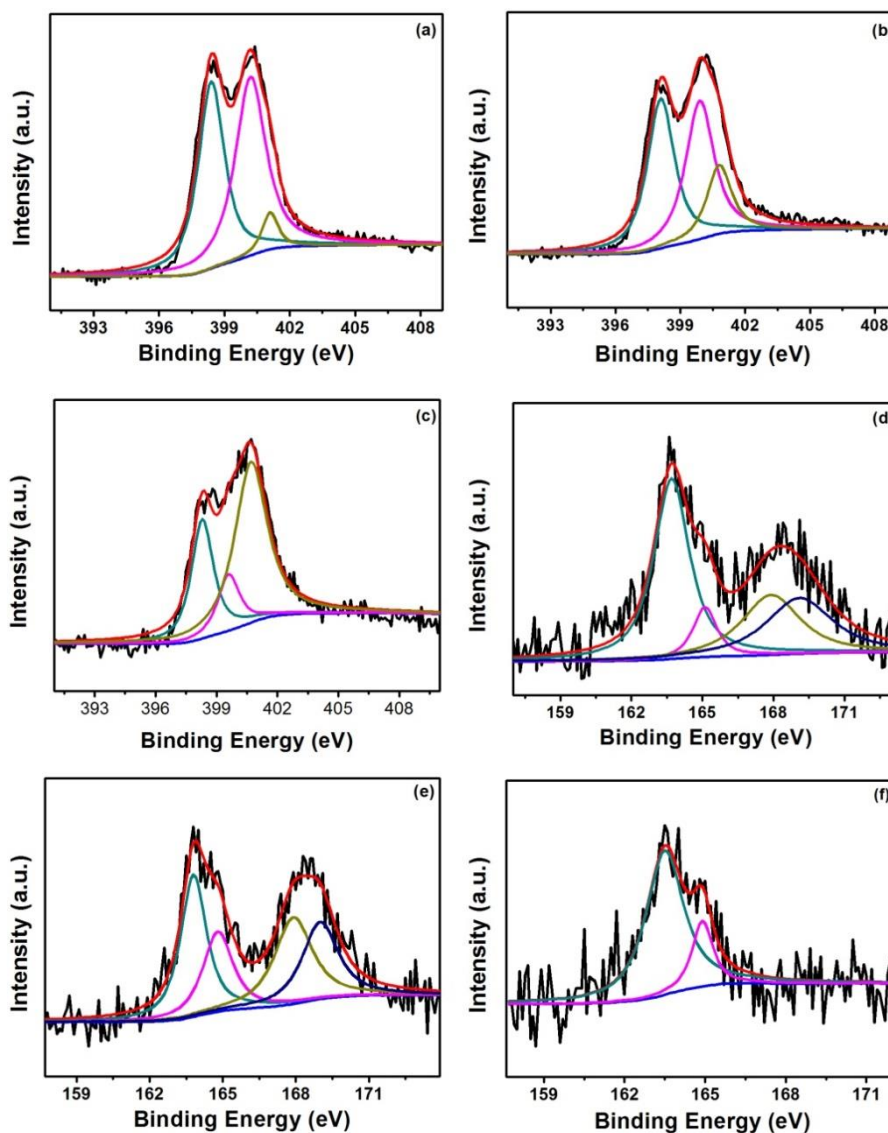


**Figure S1.** Peak deconvolutions of the (a-c) N1s and (d-f) S2p spectra of HPC-600, HPC-700, HPC-800 and HPC-900.

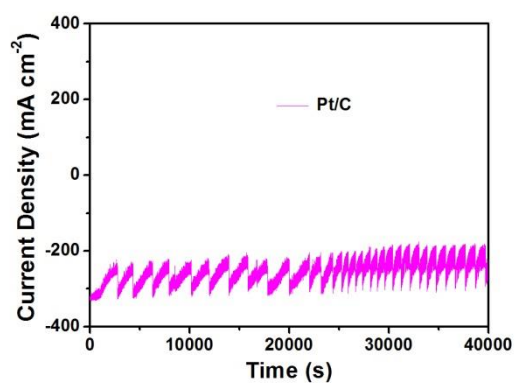


**Figure S2.** Current–time plots of HER catalyzed by 20 wt% Pt/C at the applied potential of -0.15 V (vs RHE) in 0.5 M H<sub>2</sub>SO<sub>4</sub>.

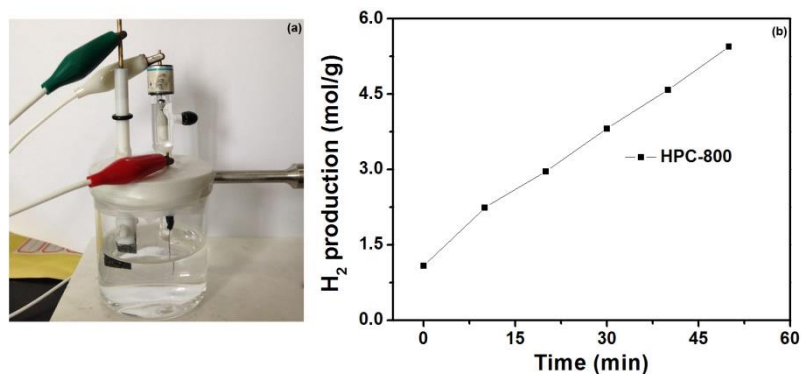


**Figure S3.** (a) Bubble formation on the HPC-800 at the applied potential of  $-0.15$  V (vs. RHE). (b) Production of hydrogen gas normalized by the weight of the HPC-800 at different reaction time.

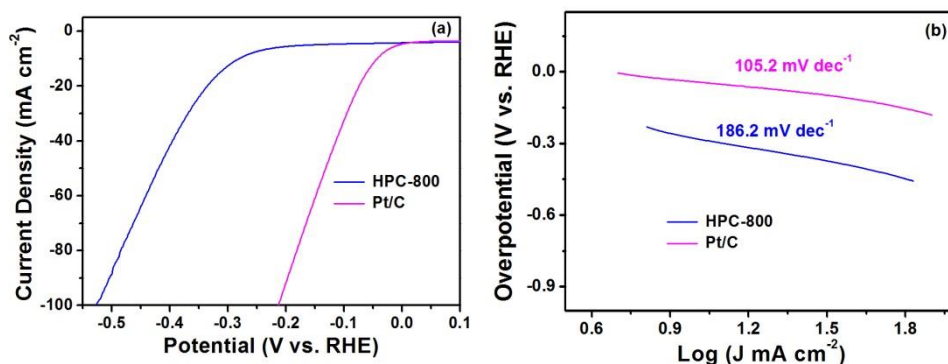


**Figure S4.** (a) Polarization curves for HER in 1 M KOH at HPC-800. Potential sweep rate 5 mV/s. (b) Corresponding Tafel plots (overpotential versus log current density) derived from (a).

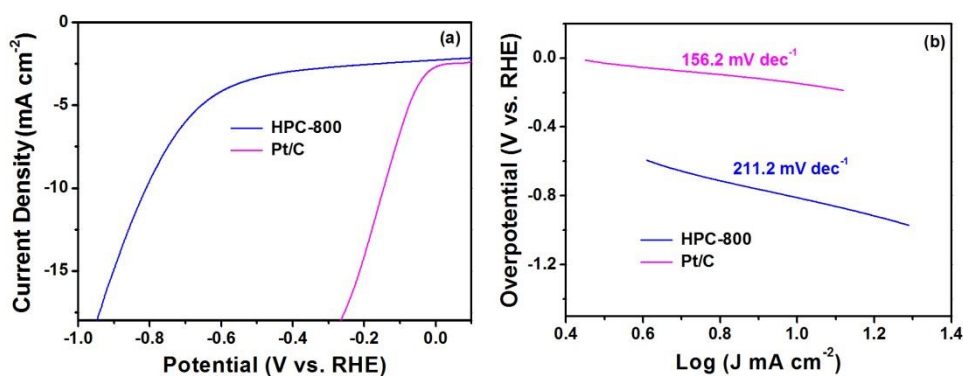


**Figure S5.** (a) Polarization curves for HER in 0.1 M phosphate buffer at HPC-800. Potential sweep rate 5 mV/s. (b) Corresponding Tafel plots (overpotential versus log current density) derived from (a).

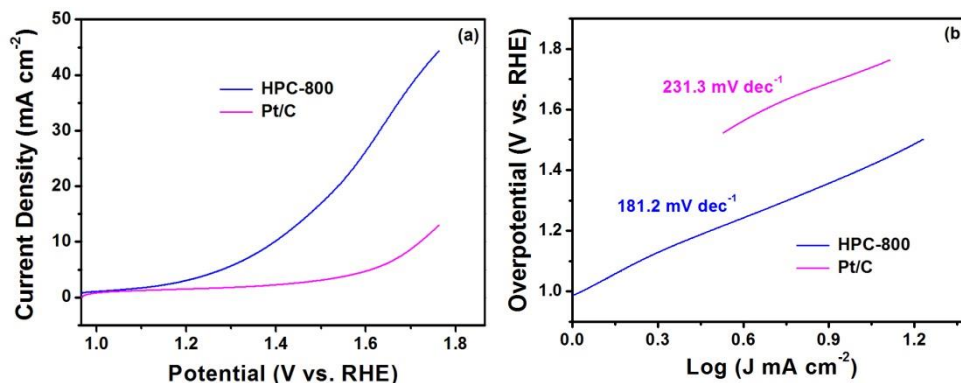


**Figure S6.** (a) Polarization curves for oxygen evolution reaction (OER) in 1 M KOH at HPC-800. Potential sweep rate 5 mV/s. (b) Corresponding Tafel plots (overpotential versus log current density) derived from (a).

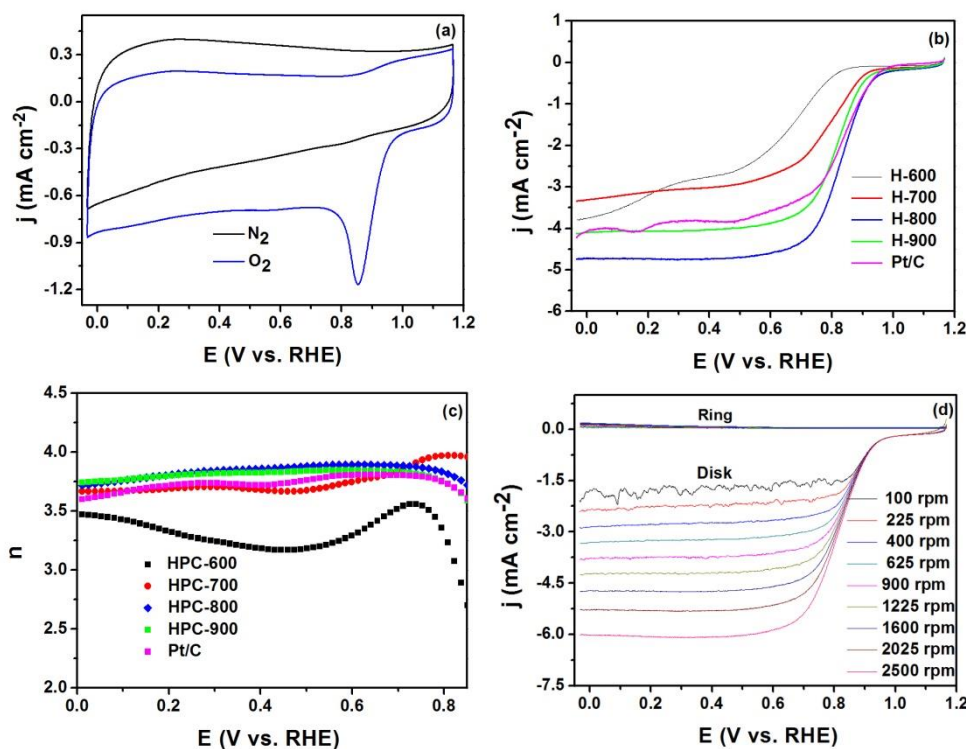


**Figure S7.** (a) CV curves of HPC-800 in N<sub>2</sub> and O<sub>2</sub>-saturated 0.1 M KOH; (b) Linear sweep voltammograms of HPC-600, HPC-700, HPC-800, HPC-900 and Pt/C RDE electrodes at 1600 rpm and 10 mV s<sup>-1</sup>; (c) The dependence of electron transfer number *n* on potential for HPC-600, HPC-700, HPC-800, and HPC-900; (d) Polarization curves for ORR in O<sub>2</sub>-saturated 0.1 M KOH solution on HPC-800 electrode at various rotation rates.

### Oxygen reduction reactions

The performance of the human derived porous carbon for ORR was measured on a rotating ring-disk electrode (RRDE) from Pine Instrument, Inc. A Pt foil and a reversible hydrogen electrode (RHE) were used as the counter electrode and reference electrode, respectively. The working electrode was a rotating ring-disk electrode with a glassy carbon disk (5.61 mm in diameter, with a collection efficiency of 37%). The working electrode was fabricated by

casting Nafion-impregnated carbon ink onto the glassy carbon disk electrode. 2.0 mg of carbon sample was added into 1 mL ethanol and 10  $\mu\text{L}$  Nafion solution (5 wt%, Aldrich) and ultrasonicated for 30 min to form a well-dispersed ink. The ink (20  $\mu\text{L}$ ) was transferred onto the surface of the glass carbon electrode and then dried at room temperature for 20 min to obtain a catalyst thin film. Commercial Pt/C was loaded onto the electrode surface in a similar fashion. The ORR test were performed with a scan rate of 10  $\text{mV s}^{-1}$  in an  $\text{O}_2$ -saturated 0.1  $\text{mol L}^{-1}$  KOH solution at room temperature, and the geometrical area of the electrode was used to calculate the current density.

The ORR catalytic activity of HPC-800 was initially investigated using cyclic voltammetry (CV) measurements in  $\text{N}_2$ -saturated and  $\text{O}_2$ -saturated 0.1 M KOH solution at a scan rate of 10  $\text{mV s}^{-1}$ , in the  $\text{N}_2$ -saturated solution, there is no obvious redox peak observed from the CV curve, in contrast, a well-defined characteristic ORR peak starting at +0.85 V was observed when  $\text{O}_2$  were introduced (**Figure S7a**). Linear sweep voltammetry (LSV) measurements for four samples and commercial Pt/C (20 wt% Pt) were performed on a rotating disk electrode (RDE) in  $\text{O}_2$ -saturated 0.1 M KOH. As shown in **Figure S7b**, the HPC-800 presents a positive onset potential of +0.92 V very close to those of Pt/C (+0.93 V), and markedly more positive than those of HPC-600 (+0.83 V), HPC-700(+0.89 V) and HPC-900 (+0.90 V). **Figure S7c** displays the dependence of the electron transfer number on the potential obtained from the different electrodes. The calculated average  $n$  values in are of 3.33 (HPC-600), 3.72 (HPC-700), 3.84 (HPC-800), 3.81 (HPC-900), and 3.74 (Pt/C) with electrode potential in the range of 0 to +0.85V. A series of LSV curves at different rotation rates for different catalysts are shown in **Figure S7d**.

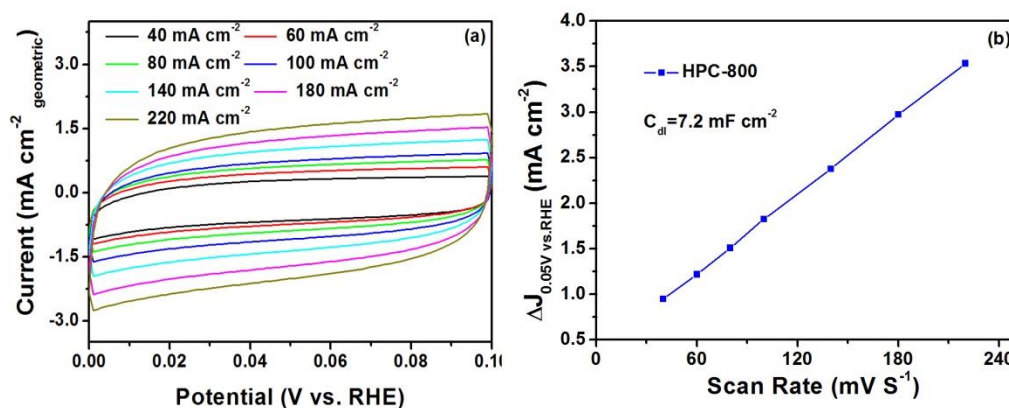


**Figure S8.** (a) Cyclic voltammograms (CV) within the range of 0 V to +0.1 V where no faradaic reactions occurred. (b) Variation of double-layer charging currents at +0.05 V with potential scan rate. Symbols are experimental data acquired from panel (a), and dotted line is linear regression.

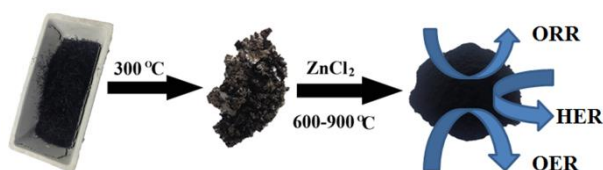


**Figure S9.** Large scale synthesis of hair derived porous carbons.